CSIRO PUBLISHING

Publications of the Astronomical Society of Australia, 2012, **29**, 115–120
http://dx.doi.org/10.1071/AS11069

AMS Applications in Nuclear Astrophysics: New Results for $^{13}C(n,\gamma)^{14}C$ and $^{14}N(n,p)^{14}C$

A. Wallner[A,B,I], *K. Buczak*[A], *I. Dillmann*[C], *J. Feige*[A], *F. Käppeler*[C], *G. Korschinek*[D], *C. Lederer*[A], *A. Mengoni*[E], *U. Ott*[F], *M. Paul*[G], *G. Schätzel*[A], *P. Steier*[A], *and H. P. Trautvetter*[H]

[A]VERA Laboratory, Faculty of Physics, University of Vienna, Austria
[B]Department of Nuclear Physics, Research School of Physics and Engineering, The Australian National University, Canberra, ACT 0200, Australia
[C]Karlsruhe Institute of Technology (KIT), Campus Nord, Institut für Kernphysik, Karlsruhe, Germany
[D]Physik Department der Technischen Universität München, Germany
[E]International Atomic Energy Agency, Nuclear Data Section, Austria
[F]Max-Planck-Institute for Chemistry, Hahn-Meitner-Weg 1, D-55128 Mainz, Germany
[G]Racah Institute of Physics, Hebrew University, Jerusalem, Israel
[H]Institut für Experimentalphysik, Ruhr-Universitaet Bochum, D-44780 Bochum, Germany
[I]Corresponding author. Email: anton.wallner@univie.ac.at, anton.wallner@anu.edu.au

Abstract: The technique of accelerator mass spectrometry (AMS) offers a complementary tool for studying long-lived radionuclides in nuclear astrophysics: (1) as a tool for investigating nucleosynthesis in the laboratory; and (2) via a direct search of live long-lived radionuclides in terrestrial archives as signatures of recent nearby supernova-events. A key ingredient to our understanding of nucleosynthesis is accurate cross-section data. AMS was applied for measurements of the neutron-induced cross sections $^{13}C(n,\gamma)$ and $^{14}N(n,p)$, both leading to the long-lived radionuclide ^{14}C. Solid samples were irradiated at Karlsruhe Institute of Technology with neutrons closely resembling a Maxwell–Boltzmann distribution for $kT = 25$ keV, and with neutrons of energies between 123 and 178 keV. After neutron activation the amount of ^{14}C nuclides in the samples was measured by AMS at the VERA (Vienna Environmental Research Accelerator) facility. Both reactions, $^{13}C(n,\gamma)^{14}C$ and $^{14}N(n,p)^{14}C$, act as neutron poisons in s-process nucleosynthesis. However, previous experimental data are discordant. The new data for both reactions tend to be slightly lower than previous measurements for the 25 keV Maxwell–Boltzmann energy distribution. For the higher neutron energies no previous data did exist for $^{13}C(n,\gamma)$, but model calculations indicated a strong resonance structure between 100 and 300 keV which is confirmed by our results. Very limited information is available for $^{14}N(n,p)$ at these energies. Our new data at 123 and 178 keV suggest lower cross sections than expected from previous experiments and data evaluations.

Keywords: techniques: miscellaneous — nuclear reactions, nucleosynthesis, abundances

Received 2011 November 30, accepted 2012 March 21, published online 2012 May 2

1 Introduction

Nuclear data provide a key ingredient for nucleosynthesis calculations and for our understanding of the chemical evolution in our galaxy. Accelerator mass spectrometry (AMS) is a relatively new technique which can be applied for measuring cross sections of relevance to nucleosynthesis. For specific reactions the sensitivity of AMS offers a unique tool to pin down uncertainties, thus elucidating current open questions e.g. within the s- and p-process path. AMS has been introduced to laboratory experiments in nuclear astrophysics for studying production of ^{44}Ti from $^{40}Ca(\alpha,\gamma)$ (Paul et al. 2003a; Nassar et al. 2006), of ^{26}Al via $^{25}Mg(p,\gamma)$ (Arazi et al. 2006) and for neutron capture reactions in the regime of s-process environments, e.g. $^{62}Ni(n,\gamma)$ (Nassar et al. 2005a). More specifically, AMS has been applied recently for neutron-capture studies of ^{40}Ca, ^{58}Ni, ^{62}Ni, and ^{78}Se (Dillmann et al. 2009, 2010, Rugel 2007) and in a series of recently completed measurements (see e.g. Wallner et al. 2007, 2010).

AMS is also used in a different but closely related application, namely for the search of live supernova (SN)-produced radionuclides in terrestrial archives, which might be imprinted through a unique isotopic signature (Ellis, Fields & Schramm 1996; Korschinek et al. 1996). Depending on the half-life of the searched-for radionuclide, one can reach back in time a few million

Table 1. Main parameters for the neutron irradiations at KIT

Sample	Reaction	E_p	$<E_n>$	Neutron fluence
^{13}C graphite-1	^{13}C(n,γ)^{14}C	1912 keV	25 keV-RK	1.45×10^{15} n cm^{-2}
^{13}C graphite-2	^{13}C(n,γ)^{14}C	1960 keV	128 keV	6.65×10^{14} n cm^{-2}
^{13}C graphite-3	^{13}C(n,γ)^{14}C	2000 keV	167 keV	4.67×10^{14} n cm^{-2}
Uracil-1	^{14}N(n,p)^{14}C	1912 keV	25 keV-RK	8.43×10^{14} n cm^{-2}
Uracil-2	^{14}N(n,p)^{14}C	1960 keV	123 keV	8.64×10^{14} n cm^{-2}
Uracil-3	^{14}N(n,p)^{14}C	2000 keV	178 keV	6.04×10^{14} n cm^{-2}

years when searching for live ^{60}Fe ($t_{1/2} = 2.62$ Myr, Rugel et al. 2009), or several hundred million years, if searching for longer-lived radionuclides such as the pure r-process nuclide ^{244}Pu ($t_{1/2} = 81$ Myr). Indeed measurements by Knie et al. found a clear signal of extraterrestrial ^{60}Fe in a deep-sea manganese crust (Knie et al. 2004). Other measurements e.g. for SN-produced ^{244}Pu did not provide clear evidence for such a signal yet (Paul et al. 2001, 2003b, 2007; C. Wallner et al. 2004), even with improved sensitivity in ^{244}Pu detection (A. Wallner et al., in preparation). However, new technical developments and new sample material now available have triggered a series of new projects for the search of such radionuclides (Korschinek, private communication; Feige et al. 2012; Bishop et al. 2011).

Here, we present new measurements for studying neutron capture on ^{13}C and for the ^{14}N(n,p) reaction. Neutron capture cross sections on light elements are usually very low (of the order of some 10 to 100 μbarn in the keV neutron energy range). Both, ^{13}C and ^{14}N are primary nuclides which are produced by the star itself. Although the capture cross sections for ^{13}C and ^{14}N are small, their abundances are high, therefore such reactions need to be considered as potential neutron poisons for the s-process: ^{13}C(α,n) is the most important neutron source for the main s-process. While neutron capture on ^{12}C(n,γ)^{13}C will also take place simultaneously with ^{13}C(n,γ), the produced ^{13}C will serve as a target for the ^{13}C(α,n)^{16}O reaction and the neutron consumed in the preceding ^{12}C(n,γ) reaction will be recycled, and thus recovered (Iliadis 2007). This is not the case for ^{13}C(n,γ). Moreover, via this neutron capture reaction, two ingredients for s-process nucleosynthesis are removed: (1) the primary ^{13}C nuclide, which forms the target for the neutron production via ^{13}C(α,n), is transformed to ^{14}C, and (2) a neutron is also consumed and missing for s-process nucleosynthesis. For the second reaction studied in this work, ^{14}N(n,p)^{14}C, we note that the cross section is about 100 times higher (ca. 2 mbarn for keV energies) than the typical neutron capture cross sections in this mass range (ca. 10 μbarn). Furthermore, ^{14}N(n,p) produces protons which subsequently destroy ^{13}C via ^{13}C(p,γ) and form a cycle with the reaction product being again ^{14}N. As such, this reaction represents the most important neutron poison in s-process nucleosynthesis.

We investigated both reactions in the energy range around 25 keV (simulating a Maxwell-Boltzmann distribution) and at two higher neutron energies around 125 and 170 keV (see Table 1). A combination of neutron activation at Karlsruhe Institute of Technology (KIT) and subsequent AMS measurement at the University of Vienna was applied. This approach directly counts the produced ^{14}C atoms in the sample after the neutron activation rather than measuring the associated γ-radiation or the emitted protons during the irradiation.

2 Existing Data for ^{13}C(n,γ)^{14}C and ^{14}N(n,p)^{14}C

2.1 ^{13}C(n,γ)^{14}C

An interesting feature of the ^{13}C(n,γ)^{14}C reaction is a strong resonance at $E_n = 143$ keV (see Figure 1). If the width of the resonance is broad, interference effects between the resonance and direct capture contributions need to be taken into account. This is the case for ^{13}C(n,γ)^{14}C where the resonance at 143 keV interferes with the p-wave contribution of the direct capture. Previous experimental data and a comparison with calculation for ^{13}C(n,γ)^{14}C (Herndl et al. 1999) indicate that the total capture cross section is dominated by a p-wave resonant contribution at energies above 20 keV. The non-resonant contribution is considerably lower and agrees well with the value extrapolated by the $1/v$ law from the thermal cross section (Herndl et al. 1999). At temperatures above 0.3 GK the reaction rate is dominated by the 143 keV resonance, at lower temperatures p-wave and s-wave contributions are dominant. The calculations of (Herndl et al. 1999) show a satisfactory agreement with two previous experimental data (Shima et al. 1997; Raman et al. 1990) although the energy dependence of the cross section is somewhat different. A significant discrepancy is found if the calculations of Herndl et al. are compared to the most recent evaluation of JEFF-3.1 (= EAF2003) which suggests at the resonance a cross section value 25 times higher than calculated by Herndl et al.

Only two experiments exist for ^{13}C(n,γ) for neutron energies in the keV range (Shima 1997, Raman 1990). Both experiments are consistent and they indicate a decreasing energy dependence of the cross section between ~25 and ~60 keV, in contrast to the calculations, which predict an increase due to the influence from the direct p-wave and resonance contributions (see Figure 1).

2.2 ^{14}N(n,p)^{14}C

Much more work exists for ^{14}N(n,p)^{14}C in the keV energy range (Koehler & O'Brien 1989, Brehm et al. 1988,

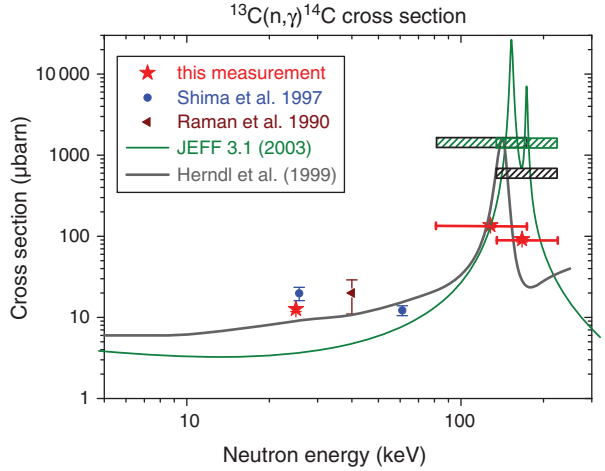

Figure 1 Experimental data for ^{13}C(n,γ)^{14}C in the keV neutron energy region. Plotted are all published experimental data and the calculated values by (Herndl et al. 1999) and recent evaluations (JEFF-3.1 and JENDL). The horizontal 'error bars' for the two experimental data at the higher energies indicate the width of the neutron energy distribution. The shaded area indicates the corresponding spectrum-averaged cross-section values for the literature values (JEFF, JENDL and Herndl et al.).

Gibbons & Barschall 1959, Johnson & Macklin 1950, Kii et al. 1999, Sanami et al. 1997). Experimental data are available for energies up to 7 MeV and there exists one additional data-point at 14.5 MeV. The measurements by (Koehler & O'Brien 1989) support a 1/v energy dependence up to some 100 keV. Other experimental data in the energy range between 10 and 200 keV show good agreement, except for a measurement by Brehm et al. (1988), which indicates cross-section values approximately a factor of two to three lower in this energy range (see Figure 2). This has a great impact on ^{14}N as a neutron poison, and also for its role on ^{19}F production, since the protons produced through ^{14}N(n,p)^{14}C play an important role in synthesizing this nuclide. While a 10% uncertainty in the ^{14}N(n,p) cross section will not have a substantial impact on ^{19}F production (Lugaro 2004, 2008), the uncertainty clearly becomes significant if one includes the data of Brehm et al.

3 Neutron Activations at KIT

Neutrons of keV energy can be produced via the ^{7}Li(p,n)^{7}Be reaction by protons impinging on a thick Li target. As this reaction has its threshold at 1881 keV, selecting a proton energy close to this threshold value generates neutrons in a forward cone with energies spread according to kinematics and energy loss in the Li target. In a proper irradiation geometry a sample can be irradiated with neutrons whose integrated cross section is directly related to a Maxwell-Boltzmann averaged cross section at an effective temperature of 25–30 keV (Ratynski & Käppeler 1988). Such a setup was developed at KIT for direct cross section measurements and for activations with subsequent decay counting of the produced activities. In this way a comprehensive set of measurements relevant to s-process nucleosynthesis was performed at KIT (see also Käppeler et al. 2011).

Samples prepared from highly enriched ^{13}C graphite powder (>98% ^{13}C) were used for studying the ^{13}C(n,γ)^{14}C reaction. The graphite powder was enclosed in small Al containers 6 mm in diameter. Au foils served as monitors for the neutron fluence determination (Ratynski & Käppeler 1988) and were attached to the ^{13}C sample to form a stack of Au-^{13}C-Au. Similarly, for the ^{14}N(n,p) studies, uracil powder ($C_4H_4N_2O_2$) was pressed into pellets and a sandwich was formed again by Au-foils. Production of ^{14}C from ^{13}C(n,γ) was negligible when using uracil due to the low ^{13}C content and the much higher ^{14}N(n,p) cross sections compared to ^{13}C(n,γ). The mass of these pellets was between 50 and 100 mg which corresponds to a thickness of 0.8 to 1.5 mm.

Three different neutron energies were selected at KIT. First, a neutron energy distribution peaking at 25 keV was produced by protons with energy $E_p = 1912$ keV (see Ratynski & Käppeler 1988). Two higher neutron energies of ~125 and ~170 keV with a broad energy spread were produced from higher-energetic protons through the same ^{7}Li(p,n) reaction (see Table 1). The experimental neutron spectrum reported by Ratynski and Käppeler is a good approximation to the experimental conditions for $E_p = 1912$ keV. The two higher neutron energy distributions, however, were simulated using the program PINO for the specific experiment (Reifarth et al. 2009). A proton beam intensity of typically 100 μA and 5 to 7 days activation resulted in a fluence of ~10^{15} neutrons per cm^2.

Table 1 lists the main parameters of the neutron activations for enriched ^{13}C and uracil samples. In Table 1, E_p denotes the proton energy in the ^{7}Li(p,n) reaction and $<E_n>$ the mean neutron energy. '25 keV-RK' means Ratynski & Käppeler distribution which relates to a Maxwell–Boltzmann distribution for $kT =$ 25 keV. 'Fluence' gives the neutron fluence for the various samples using the ^{197}Au(n,γ) cross-section value of ENDF/B-VII (Chadwick et al. 2011) and the corresponding spectral distributions (±3%). Note, a different mean neutron energy for the same proton energy may result due to a slightly different irradiation geometry.

4 Accelerator Mass Spectrometry Measurements

Accelerator Mass Spectrometry (AMS) represents a mass spectrometric technique based on the use of a (tandem) accelerator. The advantage of AMS compared to other mass spectrometric techniques is that it does not suffer from molecular isobaric interferences due to the use of tandem accelerators and can even be used for separating specific atomic isobars. It offers a complementary tool to measure cross sections of nuclear reactions leading to radioactive nuclides, independent of their decay times or schemes. The AMS measurements have been performed at the Vienna Environmental Research Accelerator (VERA) which represents a state-of-the-art AMS facility based on a 3-MV tandem (Steier et al. 2005). VERA

Table 2. Isotope ratios $^{14}C/^{13}C$ and $^{14}C/^{12}C$ as measured via AMS

Reaction	$<E_n>$	$^{14}C/^{13}C$_AMS	σ_{exp} (μbarn)
$^{13}C(n,\gamma)^{14}C$	25 keV-RK	$(1.84 \pm 0.21) \times 10^{-14}$	12.7 ± 1.5
	128 keV	$(9.1 \pm 0.6) \times 10^{-14}$	137 ± 9
	167 keV	$(4.3 \pm 0.3) \times 10^{-14}$	92 ± 7
Reaction	$<E_n>$	$^{14}C/^{12}C$_AMS	σ_{exp} (mbarn)
$^{14}N(n,p)^{14}C$	25 keV-RK	$(6.9 \pm 0.6) \times 10^{-13}$	1.66 ± 0.15
	123 keV	$(3.5 \pm 0.2) \times 10^{-13}$	0.83 ± 0.07
	178 keV	$(2.6 \pm 0.2) \times 10^{-13}$	0.88 ± 0.07

provides the ability for quantitative detection of nuclides over the whole mass range. Among the measured radioisotopes are ^{10}Be, ^{14}C, ^{26}Al, ^{36}Cl, ^{41}Ca, ^{55}Fe, ^{68}Ge, ^{129}I, ^{182}Hf, ^{202g}Pb, ^{210m}Bi, ^{229}Th, ^{231}Pa, ^{236}U and $^{239–244}Pu$, within a wide range of applications – e.g. from archaeology to climate research. In particular, since a few years nuclear astrophysics measurements are one of the main applications at VERA.

Sample material is sputtered in an ion source and specific ions are selected through a series of filters which are tuned for a specific mass, particle energy and velocity. In combination with use of negative ions and the suppression of molecules by applying acceleration and charge exchange to positive ions, AMS offers an excellent sensitivity. The actually measured quantity in AMS is an isotope ratio, i.e. rare isotope versus stable isotope contents in a sample. Basically, it measures isotope count rates for different isotopes. To this end, sequentially, stable ion currents are measured with Faraday cups, positioned at the low-energy (negative ions) and high-energy (positive ions after passing an accelerator and analyzing magnet) sides of the AMS beamline. These current measurements are alternated with counting the rare isotope with the particle detector. With this raw data, i.e. count-rate and particle current, an isotope ratio is calculated. For quality control, the transmission is regularly monitored by means of standards with well-known isotope ratios. In order to quantify or check the background level, blank samples are measured, too. Detection limits of 10^{-15} and below have been achieved for several nuclides which allow the detection of cosmogenic isotopes at natural concentrations.

Decay counting becomes difficult in case of long-lived reaction products. However, as the technique of AMS does not measure decays, but directly the number of produced radionuclides, it adds as an additional method for such measurements involving longer-lived radionuclides. Because this method is completely independent of other techniques AMS measurements provide important information on potential systematic uncertainties of previous measurements.

^{14}C AMS measurements are routinely performed in most AMS laboratories (e.g. for ^{14}C-dating). However, the samples from the neutron activations are different from above mentioned routine measurements: the ^{13}C graphite samples were about 10 000 times higher in the isotope ratio $^{13}C/^{12}C$ than natural samples (ca. 1% ^{13}C abundance in natural samples). Therefore, reference materials originating from the same ^{13}C graphite were produced from neutron activation at thermal energies. In this way we were able to study possible mass fractionation effects in the measurements which could lead to a systematic offset of the measured isotope ratio for such enriched materials. Also, the highly enriched ^{13}C sample produced a slightly higher AMS measurement background compared to data obtained from natural graphite (which is assumed to be ^{14}C free). We could demonstrate that the amount of ^{13}C produced in our neutron activated samples was high enough and background effects did not contribute to our final uncertainties (Wallner 2008, 2010). Moreover, while the ^{13}C graphite could directly be used for the AMS measurement, the uracil samples ($^{14}N(n,p)^{14}C$) required sample processing to produce graphite powder for the subsequent AMS measurement.

5 Results

Table 2 lists the measured $^{14}C/^{13}C$ and $^{14}C/^{12}C$ isotope ratios for the various neutron activated samples.

If we compare these values with typical measurement backgrounds in ^{14}C-AMS (a background of $^{14}C/^{12}C$ $\sim 3 \times 10^{-16}$ for unprocessed and $\sim 10^{-15}$ for processed samples; and similar values for the un-irradiated ^{13}C graphite samples), it is evident that background will not introduce a significant uncertainty contribution. However, other effects, most importantly some potential outgassing of freshly produced ^{14}C if converted to ^{14}CO, could not be excluded a priori. We performed a series of tests which confirmed that there were negligible losses. We have also considered a possible contamination of ^{13}C with ^{14}N: a small amount of ^{14}N could significantly contribute to ^{14}C production as its cross section is two to three orders of magnitude higher than for $^{13}C(n,\gamma)$. We have activated the same ^{13}C material with thermal neutrons and compared our results with literature values. The cross-section ratio for $^{14}N(n,p)/^{13}C(n,\gamma)$ is an order of magnitude higher for thermal neutrons (1.93 barn versus 1.4 mbarn) than e.g. for 25 keV (1.7 mbarn versus 12.7 μbarn). We have not found any enhanced cross-section value for $^{13}C(n,\gamma)$ for thermal energies, therefore one can safely assume that there is

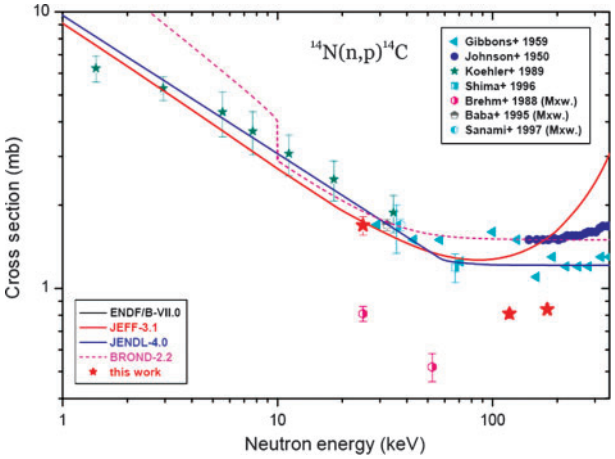

Figure 2 Experimental data and recent evaluations for ^{14}N(n,p) in the neutron energy range between 1 and 350 keV. The width of the neutron energy distributions is similar to the case of ^{13}C(n,γ).

no ^{14}N(n,p) contribution to the ^{14}C production for the higher keV neutron energies, too. More details on the AMS measurements will be published elsewhere.

The experimental cross sections σ_{exp} can simply be calculated from the following equations

$$\sigma_{exp} = \frac{^{14}C}{^{13}C} \times \frac{1}{\Phi} \quad (1)$$

and

$$\sigma_{exp} = \frac{^{14}C}{^{14}N} \times \frac{1}{\Phi}, \quad (2)$$

where ^{14}C/^{13}C and ^{14}C/^{14}N denote the isotope ratios measured via AMS, respectively, and Φ the neutron fluence. The latter was determined with an uncertainty of ±3% from Au monitor foils via ^{197}Au(n,γ) where the experimental neutron energy distributions (Ratynski & Käppeler distribution for '25 keV', and the simulated distributions around 125 and 170 keV) were folded with the cross-section data for Au(n,γ) using the values given in ENDF/B-VII. Note, the actual measured isotope ratio for ^{14}N(n,p)^{14}C is the ratio ^{14}C/^{12}C, which is directly correlated to the number of ^{14}N atoms, as for uracil ($C_4H_4N_2O_2$) ^{12}C/^{14}N = 1.98 (99% ^{12}C, 1% ^{13}C) and therefore, the AMS results are all mass independent. The broad neutron energy distributions, specific for the various activations, were modelled and the experimental data compared to existing evaluations by folding the energy distribution with these evaluated cross section data.

In Figure 1 our data (stars) for ^{13}C(n,γ)^{14}C are plotted in comparison with calculations (Herndl et al. 1999, grey line), two evaluations (JEFF-3.1, and JENDL/HE-2007) and previous experimental results (Shima et al. 1999, Raman et al. 1990). Our data indicate a good agreement with previous data for 25 keV while JEFF-3.1 is about a factor of two lower. A different picture was obtained for the two higher neutron energies with JEFF and Herndl et al. both significantly higher (~10 times). The results for the spectrum-averaged data for JEFF and Herndl et al. are indicated by the shaded area where the horizontal extension indicated the relevant neutron energy range for the two experiments, respectively.

The new spectrum-averaged cross-section data for ^{14}N(n,p) (stars) are plotted in Figure 2 together with previous experimental data and semi-empirical evaluations. At 25 keV we find a value slightly lower but close to recent experimental results and reproduces JEFF-3.1 (which is identical to ENDF/B-VII). Thus our results do not lend support to the data published by Brehm et al. (1988). At the higher neutron energies at 123 and 178 keV, respectively, our data suggest a factor of two lower values as reported from the two previous experiments (Johnson & Barschall 1950, Gibbons & Macklin 1959) indicate. Spectrum-averaged cross sections for JEFF-3.1 (= ENDF/B-VII) and JENDL-4.0 are 60% and 50% higher at 123 keV; and 70% and 40% higher at 178 keV, respectively.

6 AMS and Nuclear Astrophysics: Summary and Outlook

Recent AMS measurements have provided data that help to address open questions in nuclear astrophysics (e.g. Nassar et al. 2005b; Dillmann et al 2010; for a summary of recent AMS measurements see Wallner 2010). In the present work we exemplified this technique via measurements of the ^{13}C(n,γ) and ^{14}N(n,p) reactions. Samples containing ^{13}C and ^{14}N were irradiated at Karlsruhe Institute of Technology with neutrons having an energy distribution allowing the direct determination of a Maxwellian-averaged cross section, and also with broad neutron energy distributions between 123 and 178 keV mean energy. After the neutron activation the amount of ^{14}C produced was quantitatively determined by AMS. Both, the ^{13}C(n,γ)^{14}C and ^{14}N(n,p)^{14}C reactions act both as neutron poisons in s-process nucleosynthesis, while ^{14}N(n,p) also serves as a proton donator, leading to a delayed neutron recycling. Also the protons released in this reaction are important for the production of ^{19}F. The new data obtained for ^{13}C(n,γ) at 25 keV agree well with previous data in this energy range, while first experimental results for 128 and 167 keV neutron energy confirm the existence of a resonance as predicted by calculation, however with lower strength. The new cross section data obtained with AMS for ^{14}N(n,p)^{14}C are slightly lower at 25 keV, but significantly lower at the higher neutron energies of 123 and 178 keV than most previous experimental results. Additional AMS measurements were performed recently at VERA for the neutron capture reactions ^{9}Be(n,γ), ^{35}Cl(n,γ), ^{54}Fe(n,γ) and ^{209}Bi(n,γ).

In another approach AMS provides a sensitive technique to search for live radionuclides in terrestrial archives (Knie et al. 2004, Paul et al. 2007). AMS will also play an important role within the European Eurogenesis Research Programme 'Cosmic Dust as a Diagnostic for Massive Stars' (CoDustMas). This project comprises the laboratory study of cosmic dust via AMS measurements at University of Vienna, TU Munich, ETH Zurich,

MPI Mainz, Hebrew University, and the Australian National University (Canberra). Two aspects are investigated within this project: (1) the measurement of trace element isotope ratios in presolar nanodiamonds isolated from meteorites (stardust), e.g. isotope ratios of Pt isotopes to extract r-process nucleosynthesis signatures (Ott et al. 2012, Wallner et al. 2012); and (2) the search for live supernova (SN)-produced radionuclides in terrestrial deep-sea archives (Feige et al. 2012).

Acknowledgment

This work was partly funded by the Austrian Science Fund (FWF), project No. P20434 and I428 within the Eurocores/Eurogenesis program 'CodustMas'.

References

Arazi, A., et al., 2006, PhRvC, 74, 025802
Bishop, J. & Egli, R., 2012, Icar, 212, 960
Brehm, K., et al., 1988, ZA, 330, 167
Dillmann, I., et al., 2009, PhRvC, 79, 065805
Dillmann, I., et al., 2010, NIMPB, 268, 1283
Ellis, J., Fields, B. D. & Schramm, D. N., 1996, ApJ, 470, 1227
Chadwick, M. B., et al., 2011, NDS, 112, 2887
Feige, J., et al., 2012, PASA, Special Issue on Astronomy with Radioactivities
Gibbons, J. H. & Macklin, R. L., 1959, PhRv, 114, 571
Herndl, H., Hofinger, R., Jan, J., Oberhummer, H., Görres, J., Wiescher, M., Thielemann, F. K. & Brown, B. A., 1999, PhRvC, 60, 064614
Iliadis, C., 2007, Nuclear Physics of Stars (Weinheim: Wiley-VCH Verlag GmbH & Co. KGaA), 518
Johnson, C. H. & Barschall, H. H., 1950, PhRv, 80, 818
Käppeler, F., Gallino, R., Bisterzo, S. & Aoki, W., 2011, RvMP, 83, 157
Kii, T., Shima, T., Sato, H., Baba, T. & Nagai, Y., 1999, PhRvC, 59, 3397
Knie, K., et al., 2004, PhRvL, 93, 171103
Koehler, P. E. & O'Brien, H. A., 1989, PhRvC, 39, 1655
Korschinek, G., et al., 1996, Radiocarbon, 38, 68
Lugaro, M., et al., 2004, ApJ, 615, 934
Lugaro, M., et al., 2008, A&A, 484, 27
Nassar, H., et al., 2004, NuPhA, 746, 613
Nassar, H., et al., 2005a, PhRvL, 94, 092504
Nassar, H., et al., 2005b, NuPhA, 758, 411
Nassar, H., et al., 2006, PhRvL, 96, 041102
Ott, U., et al., 2012, PASA, Special Issue on Astronomy with Radioactivities
Paul, M., et al., 2001, ApJL, 558, 133
Paul, M., et al., 2003a, NuPhA, 718, 239
Paul, M., et al., 2003b, NuPhA, 719, C29
Paul, M., et al., 2007, JRNC, 272, 243
Raman, S., Igashira, M., Dozono, Y., Kitazawa, H. & Lynn, J. E., 1990, PhRvC, 41, 458
Ratynski, W. & Käppeler, F., 1988, PhRvC, 37, 595
Reifarth, R., Heil, M., Käppeler, F. & Plag, R., 2009, NIMPA, 608, 139
Rugel, G., et al., 2007, NIMPB, 259, 683
Rugel, G., et al., 2009, PhRvL, 103, 7
Sanami, T., et al., 1997, NIMPA, 394, 368
Shima, T., Watanabe, K., Irie, T., Sato, H. & Nagai, Y., 1995, NIMPA, 356, 347
Shima, T., Okazaki, F., Kikuchi, T., Kobayashi, T., Kii, T., Baba, T., Nagai, Y. & Igashira, M., 1997, NuPhA, 621, 231
Steier, P., et al., 2005, NIMPB, 240, 445
Wallner, A., 2010, NIMPB, 268, 1277
Wallner, C., Faestermann, T., Gerstmann, U., Knie, K., Korschinek, G., Lierse, C. & Rugel, G., 2004, NewAR, 48, 145
Wallner, A., et al., 2007, NIMPB, 259, 677
Wallner, A., et al., 2008, JPhG, 35, 014018
Wallner, A., et al., 2012, NIMPB, in press